Am J Transl Res 2020;12(6):3078-3088
www.ajtr.org /ISSN:1943-8141/AJTR0108511

Original Article

Senolytic controls bone marrow mesenchymal stem cells fate improving bone formation

Dianying Zhang[1*], Kai Yu[2*], Jie Yang[2], Shangding Xie[2], Jian Yang[2], Li Tan[2]

[1]*Department of Orthopedics and Trauma, People's Hospital, Peking University, Beijing 100044, China;*
[2]*Department of Orthopedics, Tianjin Fifth Central Hospital, Tianjin 300450, China.* [*]*Equal contributors.*

Received January 30, 2020; Accepted June 3, 2020; Epub June 15, 2020; Published June 30, 2020

Abstract: Bone marrow mesenchymal stem cells (BMSCs) are multipotential stem cells. Osteoporosis is an age-related disorder characterized by increased marrow fat accumulation and declined bone formation. Aging is an important initial factor of bone mass loss. So, manipulating the senescence of BMSCs is a considerable therapeutic target for osteoporosis treatment. To investigate the role of senolytics on regulating the differential fate of senescent BMSCs. Rat BMSCs were isolated and identified by immunofluorescence and multilineage differentiation assay. Quercetin was used to clean senescent BMSCs. Cell counting kit-8 (CCK-8) and colony formation assay was used to evaluate the cellular proliferation. While the cellular migration was detected by the scratch wound healing assay and transwell assay. And the osteogenesis assay and adipogenesis assay were used to determine the differential fate of BMSCs. BMSCs exhibited stemness. Eliminating senescent BMSCs improved the proliferation of BMSCs. But the quercetin treatment made no difference in cellular migration. And the osteogenic potential was increased while the adipogenic potential was decreased when the senescent BMSCs were cleaned by quercetin treatment. Our results demonstrate that cleaning senescent BMSCs improves the proliferation and osteogenesis of BMSCs as well as inhibits the adipogenesis of BMSCs, which provides a novel therapeutic target for the treatment of osteoporosis.

Keywords: Senolytic, senescence, osteoporosis, bone marrow mesenchymal stem cells, quercetin

Introduction

As is known to all, bone marrow mesenchymal stem cells (BMSCs) are the multipotential stem cells with the capacity to differentiate into osteoblasts, adipocytes, and chondrocytes [1, 2]. Osteoporosis is an age-related disorder characterized by increased marrow fat accumulation and declined bone formation [3-6]. It has been reported that the BMSCs collected from the elderly patients present decreased potential to differentiate into osteoblasts as well as the increased potential to differentiate into adipocytes [4, 6]. There are some studies aimed to manipulate the differential fate of senescent BMSCs to deal with this problem [7-9]. But the previous studies have majorly focused on the molecular mechanisms of signaling transduction in the BMSCs. Many studies have demonstrated that the accumulation of DNA damage and other cellular stressors [10-13] would cause various cells, including proliferating cells [14, 15], terminally differentiated cells, to undergo senescence [16-19], which was characterized by secretome changes and profound chromatin. It has been reported that the low abundance of senescent cells is sufficient to lead tissue dysfunction [20]. Farr et al [16] have reported that various cell types in the bone marrow microenvironment undergo senescence with aging. And it has been demonstrated that the expression of a well-known senescent marker, P16, was increased significantly in the osteocytes isolated from the old mice, accompanied by the accelerated age-relative bone loss [21, 22]. Eliminating senescent cells by the senolytics administration has been demonstrated to be an effective approach to extend health pan, delay the development of various age-related morbidities in multiple age mice model, including normal, chronologically and progeroid aged mice [23-26]. Especially, Farr et al [24] used the combination of dasatinib and quercetin to locally clean senescent cells in the bone marrow to attenuate age-related bone loss by suppressing the activity of bone resorp-

tion by osteoclasts. So the senescence-based therapeutic strategy would be a promising approach for osteoporosis treatment. But the differential fate of BMSCs was not investigated in the study of Farr et al [24]. The balance between bone resorption and bone formation is necessary to maintain bone mass. More and more evidence has demonstrated that the interaction between BMSCs-osteoblasts and monocyte-macrophage-osteoclasts plays an important role in the development of osteoporosis. And senescent cells can synthesize and secret the senescence-associated secretory phenotype (SASP) into the bone marrow microenvironment. The SASP would inhibit osteogenesis and promote adipogenesis of BMSCs, which has been considered as an important cause of bone loss in osteoporosis. According to the above findings, we propose a hypothesis that eliminating senescent BMSCs change the differential fate of BMSCs that upregulating the osteogenesis as well as downregulating the adipogenesis. Herein, we isolated and identified rat BMSCs, and used quercetin to clean senescent MSCs. Osteogenesis assay and adipogenesis assay were performed to evaluate the osteogenic and adipogenic potential of BMSCs to verified our hypothesis.

Materials and methods

Animals

All animal procedures were subject to approval by the animal ethics committee of Nanjing Medical University. A set of 3-week-old (50-60 g) male Sprague-Dawley rats was provided by the Animal Experiment Center of Peking University. This study was approved by the Animal Ethics Committee of Peking University Animal Center.

MSCs isolation

The 3-week-old rats were sacrificed humanely by overdose anesthesia. The bone marrow of the tibia and the femur were harvested by flushing using the 0.01 M phosphate-buffered saline (KGB5001, Keygen Biotech, Nanjing, China). Then the cells were transferred to the 50 mL tube and centrifuged at 450 g for 5 min. Then the pellets were resuspended in 10 mL dulbecco's modified eagle medium/F12 (DMEM/F12) + medium (KGM12500S-500, Keygen Biotech, Nanjing, China) containing 10% fetal calf serum (HyClone, South Logan, UT, USA). The cells were seeded in the dished and the culture medium was not changed until the nucleated cells adhered. Subsequently, the culture medium was changed every 3 days and the cells were passaged by trypsin before colonies become multilayered. The primary, passage 1 (P1), and passage 15 BMSCs were utilized for further experiments. The passage 15 CPCs were randomly divided into three groups: Control group (P15), vehicle group (Veh), and quercetin treatment group (Q).

Immunofluorescence staining

The BMSCs cultured in the 24-well plates were fixed with 4% paraformaldehyde for 20 minutes. The simples were blocked. Subsequently, the BMSCs were incubated with the primary antibodies against OCT4 (1:100, ab18976, abcam, Cambridge, MA, USA), Sry related HMG box (SOX) 2 (ab79351, 1:200, abcam, Cambridge, MA, USA), Nanog (1:200, ab106465, abcam, Cambridge, MA, USA) at 4°C overnight followed by incubation with Alexa Fluor488-preadsorbed goat anti-rabbit IgG (ab150077, Abcam, 1:500, Cambridge, MA, USA) for 2 hours at room temperature. Finally, we used the 4',6-diamidino-2-phenylindole (DAPI) Fluoromount-G (0100-20, SouthernBiotech, Birmingham, AL, USA) to mount the sections for 1 h at 4°C. The staining BMSCs were inspected with the inverted fluorescence microscope (MF53-HG, Mshot, Guangzhou, China).

Quercetin treatment

To generate the stock solution, we dissolved 33.8 mg quercetin per milliliter of dimethyl sulfoxide (DMSO). Then 1 μL stock solution was diluted in 1 ml medium to get the final concentration. The BMSCs in the P15+Q group were incubated with quercetin for 24 h. And the BMSCs in the Veh group were treated with an equal volume of DMSO.

Multilineage differentiation assay

Chondrogenesis assay was performed by using the chondrogenic induction medium (RASMX-90041, Cyagen, Guangzhou, China) according to the manufacturer's instructions. In brief, 3~4 × 10^5 BMSCs were transferred into a 15 mL EP tube. The BMSCs were centrifuged at 150 g for 10 min to form cell pellets and then the BMSCs were cultured in the chondrogenic induction medium. The cell pellets were harvested after a

Table 1. Primer sequences for qRT-PCR

Gene	Primer sequence
GAPDH	F: 5'-GTCGGTGTGAACGGATTTG-3'
	R: 5'-ACAAACATGGGGGCATCAG-3'
Osterix	F: 5'-GGGTAGTCATTTGCATAGCCAGA-3'
	R: 5'-TCTCAAGCACCAATGGACTCCT-3'
RUNX2	F: 5'-TGTCCTTGTGGATTAAAAGGACTT-3'
	R: 5'-TTTAGGGCGCATTCCTCATC-3'
Pparg	F: 5'-GGAAAAAACCCTTGCATCCTTC-3'
	R: 5'-TTCAAACTCCCTCATGGCCA-3'
Fabp4	F: 5'-GCGTGGAATTCGATGAAATCA-3'
	R: 5'-CCCGCCATCTAGGGTTATGA-3'

3-weeks culture. Adipogenesis and osteogenesis assay were performed by using the adipogenic induction medium (RASMX-90031, Cyagen, Guangzhou, China) and osteogenic induction medium (RASMX-90021, Cyagen, Guangzhou, China) according to the manufacturer's instructions, respectively.

Safranin-O (Saf-O) staining

The cell pellets were fixed, dehydrated and embedded into the paraffin. Then the sections of 7 μm thick were cut serially. The sections were stained with Safranin-O (Saf-O) (G1053, Servicebio, Wuhan, China) for 30 s.

β-galactosidase (β-gal) staining

The MCSs cultured in the 24-well plates were fixed with 4% paraformaldehyde for 20 minutes. Then the BMSCs were stained for β-gal using the senescence β-galactosidase staining kit (C0602, Beyotime, Shanghai, China) according to the manufacturer's instructions.

Cell counting kit 8 (CCK8) assay

Cellular proliferation was evaluated using the CCK-8 (C0038, Dojindo, Japan) according to the manufacturer's instructions. In brief, 2000 BMSCs were seeded into the 96-well plates. Then the BMSCs were incubated with 10 μL CCK8 solution for 2 h at 37°C. A microplate reader was used to determine the absorbance. CCK8 assay was performed at the day 7 after BMSCs seeding.

Scratch wound healing assay

BMSCs were seeded in the culture-inserts (80209, Ibidi, Gräfelfing, Germany) follow by cultured to nearly 100% confluence. Then the culture-insert was removed. The distance of the gaps was measured at the time points of 24 h after the inserts removing.

Transwell assay

The Boyden chamber (3422, Costar, Coppell, TX, USA) was used to perform transwell assay. 30000 BMSCs were seeded in upper chambers while the lower wells were filled with medium follow by incubated at 37°C for 24 hours. Then the BMSCs migrated to the lower surface were fixed and stained by using crystal violet staining solution (KGA229, Keygen Biotech, Nanjing, China).

Colony-forming unit assay

The cells were trypsinized as single cells in 6-well plates at a low density of 200 cells/well. After cultured in DMEM+/F12 medium for 15 days, cultures were fixed in 4% paraformaldehyde and stained with crystal violet staining solution (KGA229, Keygen Biotech, Nanjing, China), then the crystal violet positive area was quantified.

Quantitative real-time polymerase chain reaction (qRT-PCR)

We used the TRIzol reagent to isolate total RNA. Then the RNA was reverse-transcribed by using the complementary deoxyribose nucleic acid (cDNA) Synthesis Kit (WG441-K1622, Thermo, Waltham, MA, USA) according to the manufacturer's recommendations. The relative expression level of glyceraldehyde 3-phosphate dehydrogenase (GAPDH) was used as an internal reference. We performed qRT-PCR by using a 1 μL cDNA sample of each group in the 7500 Real-Time PCR System with an SYBR Green PCR Core Kit (KGA1339-1, Keygen Biotech, Nanjing, China). The qRT-PCR was performed in triplicate. The primer sequences were listed in **Table 1**. Relative quantitative analysis was performed using the $2^{-\Delta\Delta Ct}$ method. The results were presented as the fold changes compared with the control.

Statistical analysis

We used the statistical software package Statistical Product and Service Solutions (SPSS) 24.0 (IBM, Armonk, NY, USA) to perform all statistical analyses. Shapiro-Wilk test and Bartlett's test were performed. A comparison between multiple groups was done using a one-

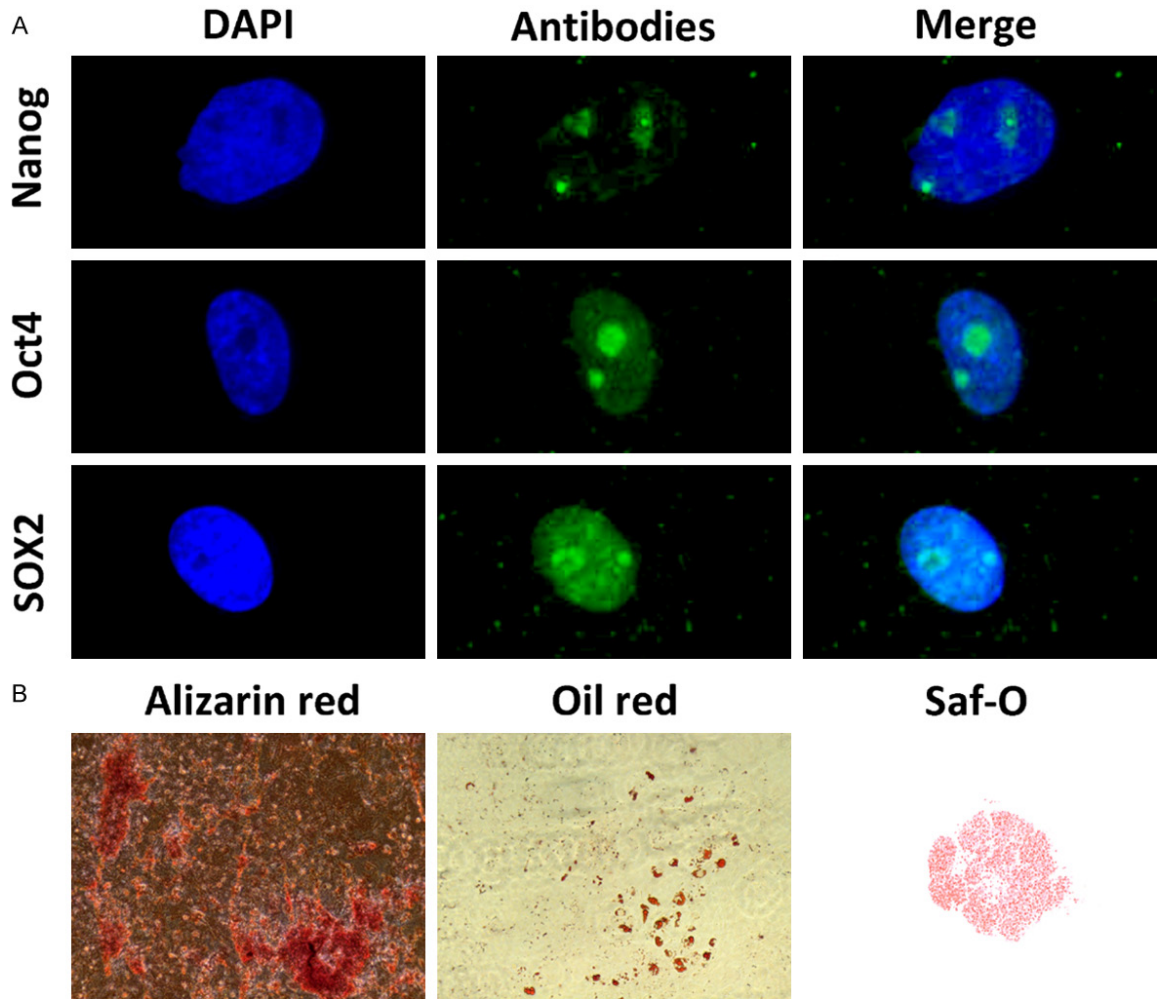

Figure 1. Identification of isolated BMSCs. A. Representative immunofluorescence staining of Nanog (green, top), Oct4 (green, middle), SOX2 (green, bottom) and DAPI (blue) of the primary BMSCs (magnification: 200×). B. Representative microscopic images of the alizarin staining for osteogenic differentiation assay (left), oil red staining for adipogenic differentiation assay (middle), Saf-O staining for chondrogenic differentiation assay (right) of the primary BMSCs (magnification: 100×).

way ANOVA test followed by Post Hoc Test (Least Significant Difference). Data were presented as mean ± SD and values of $P<0.05$ were considered significant. GraphPad Prism 7 (Graph Software, San Diego, CA, USA) was used to generate the statistic graphs.

Results

Quercetin cleaned senescent BMSCs improving the proliferation of BMSCs

We identified the stemness of BMSCs by the immunofluorescence staining and multilineage differentiation assay. First, we found that the BMSCs were positive for both Nanog, OCT4 and SOX2, the three well-known cell-renew markers (**Figure 1A**). Second, calcium nodules formation with strong alizarin red staining was observed in the osteogenesis assay (**Figure 1B**). And the isolated BMSCs were able to differentiate to adipocytes and chondrocytes as shown in the adipogenic and chondrogenic differential assay (**Figure 1B**). Subsequently, we used the quercetin to induce senescent BMSCs toward apoptosis. As shown in the β-gal staining, there were more β-gal positive BMSCs in the P15 group compared with the P1 group. And the number of β-gal positive MCSs was decreased significantly after quercetin treatment compared with the P15 group while the vehicle treatment made no differences (**Figure 2A**). Quantitative analysis of β-gal positive BMSCs also revealed the same result. Unexpectedly, the number of β-gal positive BMSCs

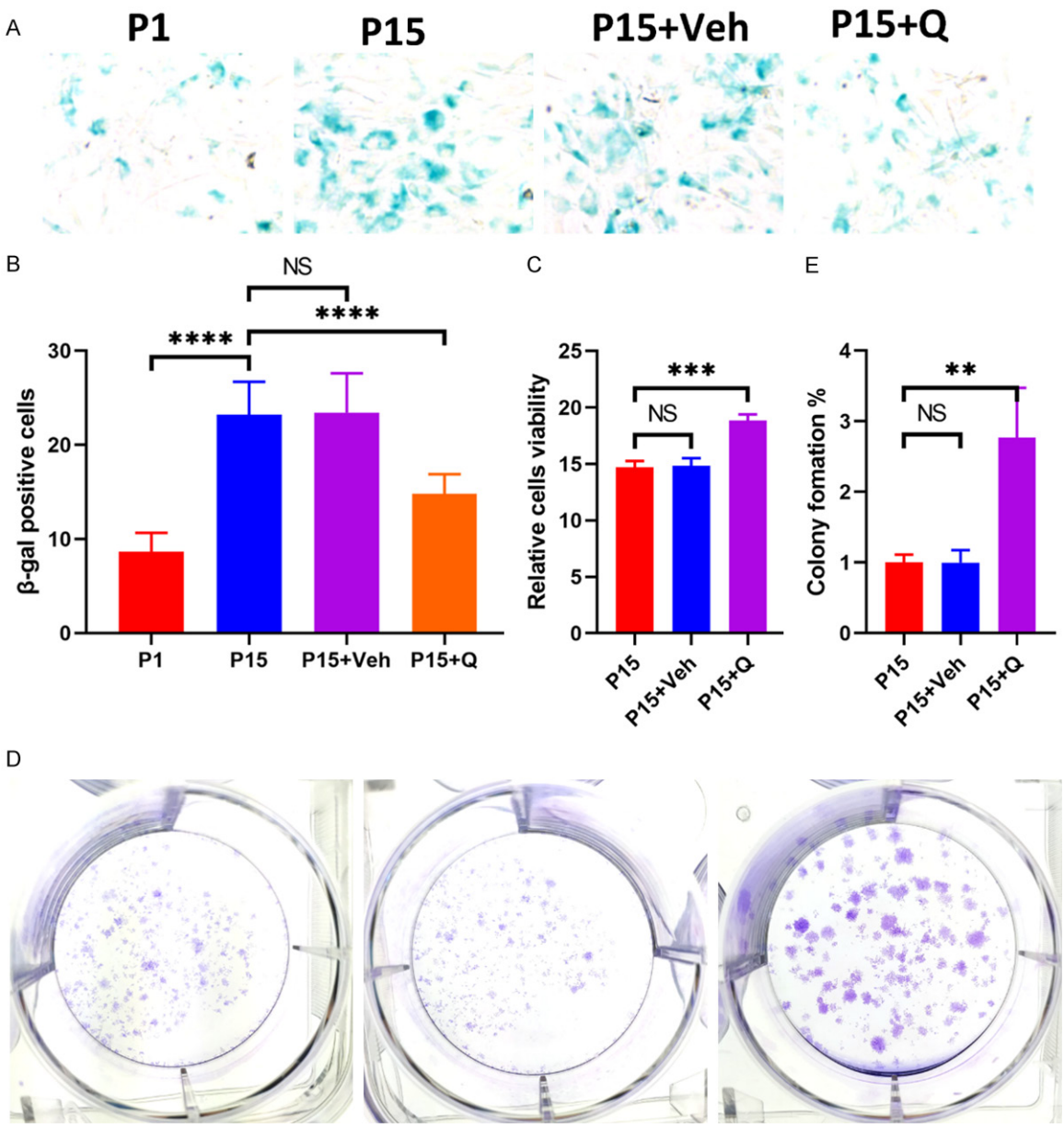

Figure 2. Quercetin cleaned senescent BMSCs improving the proliferation of BMSCs. A. Representative microscopic images of the β-gal staining of the BMSCs in the P1 group, P15 group, P15+Vel group, and P15+Q group (magnification: 400×). B. Quantitative analysis of the percentage of β-gal positive BMSCs in the P1 group, P15 group, P15+Vel group, and P15+Q group. Values are shown as mean ± SD. NS, no significance, ****P<0.0001, one-way ANOVA with Tukey's multiple comparisons test. C. CCK8 assay of the BMSCs in the P1 group, P15 group, P15+Vel group, and P15+Q group. Values are shown as mean ± SD. NS, no significance, ***P<0.001, one-way ANOVA with Tukey's multiple comparisons test. D. Representative macroscopic photos of colony formation assay of the P1 group, P15 group, P15+Vel group, and P15+Q group (magnification: 10×). E. Quantitative analysis of colony formation assay of the P1 group, P15 group, P15+Vel group, and P15+Q group. Values are shown as mean ± SD. NS, no significance, **P<0.01, one-way ANOVA with Tukey's multiple comparisons test.

was higher than that of the P1 group (**Figure 2B**). Next, the cellular proliferation was detected by CCK8 assay. We found that the proliferative BMSCs in the P15 group were decreased significantly compared to the P1 group. Quercetin treatment partially restored the proliferation of P15 BMSCs. However, there was still a statistic difference in the number of proliferative BMSCs between the P1 group and the P15+Q group (**Figure 2C**). Similar results were observed in the colony formation assay. Quercetin treatment increased the potential of colony formation of BMSCs (**Figure 2D**). Quantitative analysis showed that the intensity of

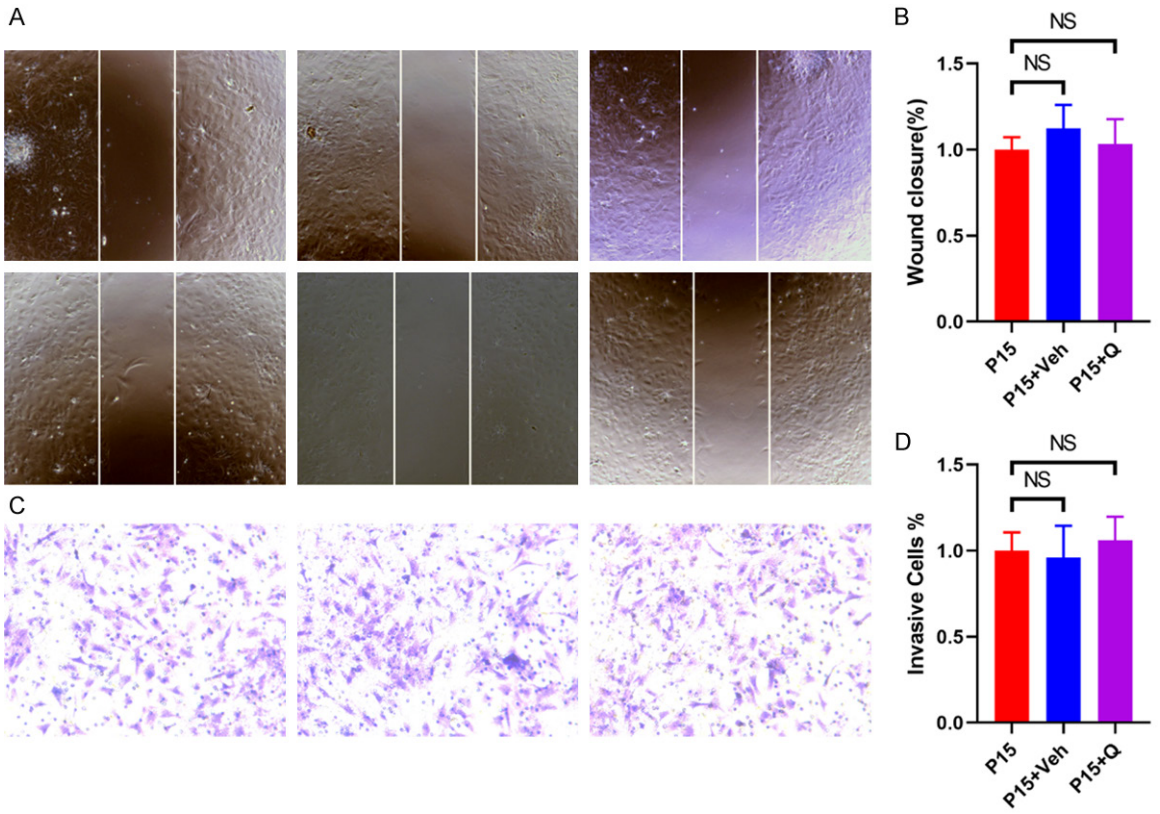

Figure 3. Eliminating senescent BMSCs did not regulate the migratory potential of BMSCs. A. Representative microscopic images of scratch wound healing of the P1 group, P15 group, P15+Vel group, and P15+Q group (magnification: 100×). B. Quantitative analysis of scratch wound healing of the P1 group, P15 group, P15+Vel group, and P15+Q group. Values are shown as mean ± SD. NS, no significance, one-way ANOVA with Tukey's multiple comparisons test. C. Representative crystal violet staining of transwell assay of the P1 group, P15 group, P15+Vel group, and P15+Q group (magnification: 400×). D. Quantitative analysis of transwell assay of the P1 group, P15 group, P15+Vel group, and P15+Q group. Values are shown as mean ± SD. NS, no significance, one-way ANOVA with Tukey's multiple comparisons test.

crystal violet was increased significantly in the P15+Q group compared with the P15 group and the P15+Veh group (**Figure 2E**).

Quercetin treatment did not regulate the migratory potential of senescent BMSCs

We found that the percentage of wound healing did not increase or decrease in the P15+Q group compared with the P15 group or the P15+Veh group (**Figure 3A**, **3B**). And the transwell assay showed the same results (**Figure 3C**, **3D**).

Eliminating senescent BMSCs improved the osteogenic potential of BMSCs

We used the osteogenic differentiation assay and qRT-PCR of the well-known osteogenic markers, Osterix and RUNX2 to evaluated the osteogenic potential of BMSCs. As expected, there were obvious calcium nodules formations in the P15+Q group, while there were only poor calcium nodules formations in the P15 group and the P15+Vel group (**Figure 4A**).

Quantitative analysis of the staining intensity of the alizarin red revealed that the highest alizarin red intensity was received in the P15+Q group (**Figure 4B**). Similarly, the results of qRT-PCR showed that the expression of Osterix and RUNX2 was increased in the P15 BMSCs after quercetin treatment compared with the P15 group, while the expression of these two osteogenic markers was not increased in the P15+Vel group (**Figure 4C**, **4D**).

Eliminating senescent BMSCs suppressed the adipogenic potential of BMSCs

Firstly, the adipogenesis assay showed that there were abundant lipid droplets in the P15 group and the P15+Vel group. And the querce-

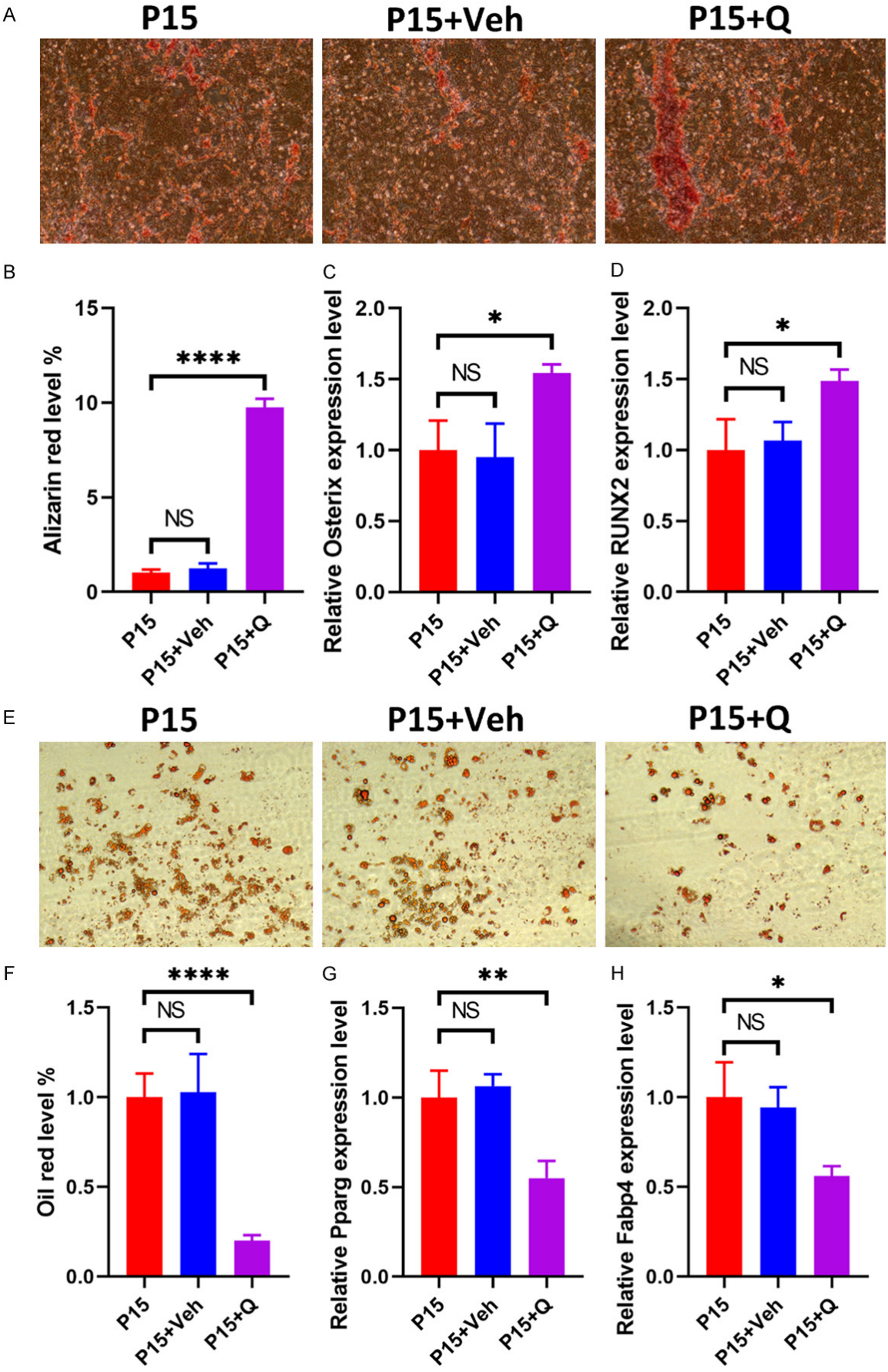
A
P15
P15+Veh
P15+Q
B
Alizarin red level %
15
10
5
0
****
NS
P15
P15+Veh
P15+Q
C
Relative Osterix expression level
2.0
1.5
1.0
0.5
0.0
*
NS
P15
P15+Veh
P15+Q
D
Relative RUNX2 expression level
2.0
1.5
1.0
0.5
0.0
*
NS
P15
P15+Veh
P15+Q
E
P15
P15+Veh
P15+Q
F
Oil red level %
1.5
1.0
0.5
0.0
****
NS
P15
P15+Veh
P15+Q
G
Relative Pparg expression level
1.5
1.0
0.5
0.0
**
NS
P15
P15+Veh
P15+Q
H
Relative Fabp4 expression level
1.5
1.0
0.5
0.0
*
NS
P15
P15+Veh
P15+Q

Figure 4. Eliminating senescent BMSCs changed the differential fate of BMSCs. A. Representative microscopic images of the alizarin red staining for the osteogenesis assay of the BMSCs in the P1 group, P15 group, P15+Vel group, and P15+Q group (magnification: 100×). B. Quantitative analysis of the intensity of the alizarin red staining for the osteogenesis assay of the BMSCs in the P1 group, P15 group, P15+Vel group, and P15+Q group. Values are shown as mean ± SD. NS, no significance, ****P<0.0001, one-way ANOVA with Tukey's multiple comparisons test. C. Analysis of the expression level of Osterix of the BMSCs in the P1 group, P15 group, P15+Vel group, and P15+Q group after osteogenic induction. Values are shown as mean ± SD. NS, no significance, *P<0.05, one-way ANOVA with Tukey's multiple comparisons test. D. Analysis of the expression level of RUNX2 of the BMSCs in the P1 group, P15 group, P15+Vel group, and P15+Q group after osteogenic induction. Values are shown as mean ± SD. NS, no significance, *P<0.05, one-way ANOVA with Tukey's multiple comparisons test. E. Representative microscopic images of the oil red staining for the adipogenesis assay of the BMSCs in the P1 group, P15 group, P15+Vel group, and P15+Q group (magnification: 100×). F. Quantitative analysis of the intensity of the alizarin red staining for the adipogenesis assay of the BMSCs in the P1 group, P15 group, P15+Vel group, and P15+Q group. Values are shown as mean ± SD. NS, no significance, ****P<0.0001, one-way ANOVA with Tukey's multiple comparisons test. G. Analysis of the expression level of Pparg of the BMSCs in the P1 group, P15 group, P15+Vel group, and P15+Q group after adipogenic induction. Values are shown as mean ± SD. NS, no significance, **P<0.001, one-way ANOVA with Tukey's multiple comparisons test. H. Analysis of the expression level of Fabp4 of the BMSCs in the P1 group, P15 group, P15+Vel group, and P15+Q group after adipogenic induction. Values are shown as mean ± SD. NS, no significance, *P<0.05, one-way ANOVA with Tukey's multiple comparisons test.

tin treatment effectively downregulated the lipid droplets formation (**Figure 4E**). Secondly, quantitative analysis showed that the intensity of oil red staining was decreased significantly in the P15+Q group compared with the P15 group and the P15+Veh group (**Figure 4F**). Finally, we found that the expression of Pparg and Fabp4 was also inhibited by quercetin treatment in the qRT-PCR assay. And vehicle treatment did not decrease the expression of Pparg and Fabp4 (**Figure 4G**, **4H**).

Discussion

BMSCs, a rare cell population, exhibit excellent stem cell potentials of multipotency and self-renewal [27]. The BMSCs have the potential of differentiation into the three mesodermal lineage cells, such as the adipocytes, the chondrocytes and the osteocytes [1, 28, 29]. We also found that the primary BMSCs expression the well-known self-renew markers (Nanog, OCT4, and SOX2) and be able to undergo osteogenesis, adipogenesis, and chondrogenesis. So the BMSCs are important in maintaining the grown skeleton and the repair of bone damage. But it has been reported that senescence impairs the activity of BMSCs that BMSCs lose their osteoblast differentiation capacity with aging [24].

Though the fate determination of BMSCs is controlled by various intrinsic and extrinsic factors, including epigenetic modification [30-32], signaling pathway [33], growth factors, mechanical induction [34, 35], and small molecules [36], which can deliver signal cues as well as activate downstream lineage-special signaling pathway and guide the differential fate commitment of BMSCs. Aging is an important initial factor of bone mass loss. So, manipulating the senescence of BMSCs is a considerable therapeutic target for osteoporosis treatment. Farr et al [24] have reported that senolytics treatment prevented age-related bone loss in aging mice through inhibiting the activity of osteoclasts by eliminating senescent cells. However, as described above, Farr et al [24] majorly focused on bone resorption. And in the present study, we investigate the role of senolytics on regulating the differential fate of senescent BMSCs. Though Farr et al [24] used the combination of dasatinib and quercetin to clean senescent cells in the bone tissue and received an ideal outcome, it has been reported that dasatinib selectively cleaned senescent preadipocytes, and quercetin selectively cleaned senescent endothelial cells and BMSCs. The combination of dasatinib and quercetin effectively eliminated senescent embryonic fibroblasts [37]. So we chose the quercetin as the senolytic in the present study to eliminate senescent rat BMSCs *in vitro*.

Quercetin treatment effectively eliminated senescent BMSCs *in vitro* as presenting in the β-gal staining, which was consistent with the findings of Farr et al [24] that the combination of dasatinib and quercetin could effectively clean P16 positive and β-gal positive cells *in vitro* and *in vivo* in the bone tissue. And we found that the proliferative potential of senescent BMSCs was increased significantly after quercetin treatment. It is consistent with the

fact that the proliferative potential of BMSCs is decreased with passaging [38]. And many studies have demonstrated that the decreased proliferation in senescent BMSCs is due to the loss of telomere length with population doubling [39, 40]. And the upregulation of proliferation of senescent BMSCs by quercetin treatment may due to the decreased secretion of SASP in the microenvironment of cell cultures [24]. Surprisingly, quercetin treatment made no difference in the migratory potential of senescent BMSCs, which was different from the results of Duscher et al [41] that hypoxia-induced migration of adipose-derived MSCs.

It has been reported that there is an imbalanced ratio of osteoblasts and adipocytes in the bone marrow in various pathological conditions, including osteoporosis and aging [33]. There are some studies aim to manipulate the differential fate of senescent BMSCs. On the one hand, Li et al [8] and Xu et al [7] rescued the osteogenic differential potential of senescent MSCs by manipulating the microRNA. On the other hand, Bolamperti et al [42] and Chen et al [43] rescued the osteogenesis of senescent MSCs by manipulating the signaling pathway. And we found that cleaning senescent BMSCs upregulated the osteogenesis as well as downregulated the adipogenesis of BMSCs, which may improve the bone mass formation. Compared with the microRNA-based therapeutic strategies and small-molecules-based therapeutic strategies, quercetin has been used clinically for a long time as the anti-cancer drug, which may be safer to be applied in the patients for osteoporosis treatment.

There are still several limitations to the present study. Firstly, we only verified the effect of senolytic on promoting bone formation *in vitro*. Secondly, the underlying mechanism by which cleaning senescent BMSCs regulates the differential fate of BMSCs needs to be explored in further studies.

Conclusion

In conclusion, our results demonstrate that cleaning senescent BMSCs by quercetin treatment improves the proliferation and osteogenesis of BMSCs as well as inhibits the adipogenesis of BMSCs. Our study may provide a novel therapeutic target for the treatment of osteoporosis, especially in elderly patients.

Disclosure of conflict of interest

None.

Address correspondence to: Dr. Dianying Zhang, Department of Orthopedics and Trauma, People's Hospital, Peking University, No. 11, Xizhimen South Street, Xicheng District, Beijing 100044, China. Tel: +86-022-65665293; E-mail: bizhuo19650918@163.com

References

[1] Pittenger MF, Mackay AM, Beck SC, Jaiswal RK, Douglas R, Mosca JD, Moorman MA, Simonetti DW, Craig S and Marshak DR. Multilineage potential of adult human mesenchymal stem cells. Science 1999; 284: 143-147.

[2] Sekiya I, Larson BL, Vuoristo JT, Cui JG and Prockop DJ. Adipogenic differentiation of human adult stem cells from bone marrow stroma (MSCs). J Bone Miner Res 2004; 19: 256-264.

[3] Yeung DK, Griffith JF, Antonio GE, Lee FK, Woo J and Leung PC. Osteoporosis is associated with increased marrow fat content and decreased marrow fat unsaturation: a proton MR spectroscopy study. J Magn Reson Imaging 2005; 22: 279-285.

[4] Shen W, Chen J, Gantz M, Punyanitya M, Heymsfield SB, Gallagher D, Albu J, Engelson E, Kotler D, Pi-Sunyer X and Gilsanz V. MRI-measured pelvic bone marrow adipose tissue is inversely related to DXA-measured bone mineral in younger and older adults. Eur J Clin Nutr 2012; 66: 983-988.

[5] Kim VN, Han J and Siomi MC. Biogenesis of small RNAs in animals. Nat Rev Mol Cell Biol 2009; 10: 126-139.

[6] Moerman EJ, Teng K, Lipschitz DA and Lecka-Czernik B. Aging activates adipogenic and suppresses osteogenic programs in mesenchymal marrow stroma/stem cells: the role of PPAR-gamma2 transcription factor and TGF-beta/BMP signaling pathways. Aging Cell 2004; 3: 379-389.

[7] Xu R, Shen X, Si Y, Fu Y, Zhu W, Xiao T, Fu Z, Zhang P, Cheng J and Jiang H. MicroRNA-31a-5p from aging BMSCs links bone formation and resorption in the aged bone marrow microenvironment. Aging Cell 2018; 17: e12794.

[8] Li CJ, Cheng P, Liang MK, Chen YS, Lu Q, Wang JY, Xia ZY, Zhou HD, Cao X, Xie H, Liao EY and Luo XH. MicroRNA-188 regulates age-related switch between osteoblast and adipocyte differentiation. J Clin Invest 2015; 125: 1509-1522.

[9] Fulzele S, Mendhe B, Khayrullin A, Johnson M, Kaiser H, Liu Y, Isales CM and Hamrick MW.

Muscle-derived miR-34a increases with age in circulating extracellular vesicles and induces senescence of bone marrow stem cells. Aging (Albany NY) 2019; 11: 1791-1803.
[10] Zhu Y, Armstrong JL, Tchkonia T and Kirkland JL. Cellular senescence and the senescent secretory phenotype in age-related chronic diseases. Curr Opin Clin Nutr Metab Care 2014; 17: 324-328.
[11] Swanson EC, Manning B, Zhang H and Lawrence JB. Higher-order unfolding of satellite heterochromatin is a consistent and early event in cell senescence. J Cell Biol 2013; 203: 929-942.
[12] LeBrasseur NK, Tchkonia T and Kirkland JL. Cellular senescence and the biology of aging, disease, and frailty. Nestle Nutr Inst Workshop Ser 2015; 83: 11-18.
[13] Tchkonia T, Zhu Y, van Deursen J, Campisi J and Kirkland JL. Cellular senescence and the senescent secretory phenotype: therapeutic opportunities. J Clin Invest 2013; 123: 966-972.
[14] Jurk D, Wilson C, Passos JF, Oakley F, Correia-Melo C, Greaves L, Saretzki G, Fox C, Lawless C, Anderson R, Hewitt G, Pender SL, Fullard N, Nelson G, Mann J, van de Sluis B, Mann DA and von Zglinicki T. Chronic inflammation induces telomere dysfunction and accelerates ageing in mice. Nat Commun 2014; 2: 4172.
[15] Campisi J and d'Adda di Fagagna F. Cellular senescence: when bad things happen to good cells. Nat Rev Mol Cell Biol 2007; 8: 729-740.
[16] Farr JN, Fraser DG, Wang H, Jaehn K, Ogrodnik MB, Weivoda MM, Drake MT, Tchkonia T, LeBrasseur NK, Kirkland JL, Bonewald LF, Pignolo RJ, Monroe DG and Khosla S. Identification of Senescent Cells in the Bone Microenvironment. J Bone Miner Res 2016; 31: 1920-1929.
[17] Minamino T, Orimo M, Shimizu I, Kunieda T, Yokoyama M, Ito T, Nojima A, Nabetani A, Oike Y, Matsubara H, Ishikawa F and Komuro I. A crucial role for adipose tissue p53 in the regulation of insulin resistance. Nat Med 2009; 15: 1082-1087.
[18] Campisi J. Senescent cells, tumor suppression, and organismal aging: good citizens, bad neighbors. Cell 2005; 120: 513-522.
[19] Jurk D, Wang C, Miwa S, Maddick M, Korolchuk V, Tsolou A, Gonos ES, Thrasivoulou C, Saffrey MJ, Cameron K and von Zglinicki T. Postmitotic neurons develop a p21-dependent senescence-like phenotype driven by a DNA damage response. Aging Cell 2012; 11: 996-1004.
[20] Herbig U, Ferreira M, Condel L, Carey D and Sedivy JM. Cellular senescence in aging primates. Science 2006; 311: 1257.
[21] Hamrick MW, Ding KH, Pennington C, Chao YJ, Wu YD, Howard B, Immel D, Borlongan C, McNeil PL, Bollag WB, Curl WW, Yu J and Isales CM. Age-related loss of muscle mass and bone strength in mice is associated with a decline in physical activity and serum leptin. Bone 2006; 39: 845-853.
[22] Glatt V, Canalis E, Stadmeyer L and Bouxsein ML. Age-related changes in trabecular architecture differ in female and male C57BL/6J mice. J Bone Miner Res 2007; 22: 1197-1207.
[23] Baker DJ, Wijshake T, Tchkonia T, LeBrasseur NK, Childs BG, van de Sluis B, Kirkland JL and van Deursen JM. Clearance of p16Ink4a-positive senescent cells delays ageing-associated disorders. Nature 2011; 479: 232-236.
[24] Farr JN, Xu M, Weivoda MM, Monroe DG, Fraser DG, Onken JL, Negley BA, Sfeir JG, Ogrodnik MB, Hachfeld CM, LeBrasseur NK, Drake MT, Pignolo RJ, Pirtskhalava T, Tchkonia T, Oursler MJ, Kirkland JL and Khosla S. Targeting cellular senescence prevents age-related bone loss in mice. Nat Med 2017; 23: 1072-1079.
[25] Xu M, Palmer AK, Ding H, Weivoda MM, Pirtskhalava T, White TA, Sepe A, Johnson KO, Stout MB, Giorgadze N, Jensen MD, LeBrasseur NK, Tchkonia T and Kirkland JL. Targeting senescent cells enhances adipogenesis and metabolic function in old age. Elife 2015; 4: e12997.
[26] Roos CM, Zhang B, Palmer AK, Ogrodnik MB, Pirtskhalava T, Thalji NM, Hagler M, Jurk D, Smith LA, Casaclang-Verzosa G, Zhu Y, Schafer MJ, Tchkonia T, Kirkland JL and Miller JD. Chronic senolytic treatment alleviates established vasomotor dysfunction in aged or atherosclerotic mice. Aging Cell 2016; 15: 973-977.
[27] Miller JP. Lecithin: cholesterol acyltransferase activity and cholestyramine resin therapy in man. Eur J Clin Invest 1976; 6: 477-479.
[28] Muraglia A, Cancedda R and Quarto R. Clonal mesenchymal progenitors from human bone marrow differentiate in vitro according to a hierarchical model. J Cell Sci 2000; 113: 1161-1166.
[29] Dominici M, Le Blanc K, Mueller I, Slaper-Cortenbach I, Marini F, Krause D, Deans R, Keating A, Prockop D and Horwitz E. Minimal criteria for defining multipotent mesenchymal stromal cells. The International Society for Cellular Therapy position statement. Cytotherapy 2006; 8: 315-317.
[30] Yin B, Yu F, Wang C, Li B, Liu M and Ye L. Epigenetic control of mesenchymal stem cell fate decision via histone methyltransferase ash1l. Stem Cells 2019; 37: 115-127.
[31] Hemming S, Cakouros D, Isenmann S, Cooper L, Menicanin D, Zannettino A and Gronthos S. EZH2 and KDM6A act as an epigenetic switch to regulate mesenchymal stem cell lineage specification. Stem Cells 2014; 32: 802-815.

[32] Ye L, Fan Z, Yu B, Chang J, Al HK, Zhou X, Park NH and Wang CY. Histone demethylases KDM4B and KDM6B promotes osteogenic differentiation of human MSCs. Cell Stem Cell 2012; 11: 50-61.
[33] Chen Q, Shou P, Zheng C, Jiang M, Cao G, Yang Q, Cao J, Xie N, Velletri T, Zhang X, Xu C, Zhang L, Yang H, Hou J, Wang Y and Shi Y. Fate decision of mesenchymal stem cells: adipocytes or osteoblasts? Cell Death Differ 2016; 23: 1128-1139.
[34] Yang C, Tibbitt MW, Basta L and Anseth KS. Mechanical memory and dosing influence stem cell fate. Nat Mater 2014; 13: 645-652.
[35] Engler AJ, Sen S, Sweeney HL and Discher DE. Matrix elasticity directs stem cell lineage specification. Cell 2006; 126: 677-689.
[36] Xu Y, Shi Y and Ding S. A chemical approach to stem-cell biology and regenerative medicine. Nature 2008; 453: 338-344.
[37] Zhu Y, Tchkonia T, Pirtskhalava T, Gower AC, Ding H, Giorgadze N, Palmer AK, Ikeno Y, Hubbard GB, Lenburg M, O'Hara SP, LaRusso NF, Miller JD, Roos CM, Verzosa GC, LeBrasseur NK, Wren JD, Farr JN, Khosla S, Stout MB, McGowan SJ, Fuhrmann-Stroissnigg H, Gurkar AU, Zhao J, Colangelo D, Dorronsoro A, Ling YY, Barghouthy AS, Navarro DC, Sano T, Robbins PD, Niedernhofer LJ and Kirkland JL. The Achilles' heel of senescent cells: from transcriptome to senolytic drugs. Aging Cell 2015; 14: 644-658.
[38] Digirolamo CM, Stokes D, Colter D, Phinney DG, Class R and Prockop DJ. Propagation and senescence of human marrow stromal cells in culture: a simple colony-forming assay identifies samples with the greatest potential to propagate and differentiate. Br J Haematol 1999; 107: 275-281.
[39] Stenderup K, Justesen J, Clausen C and Kassem M. Aging is associated with decreased maximal life span and accelerated senescence of bone marrow stromal cells. Bone 2003; 33: 919-926.
[40] Bonab MM, Alimoghaddam K, Talebian F, Ghaffari SH, Ghavamzadeh A and Nikbin B. Aging of mesenchymal stem cell in vitro. Bmc Cell Biol 2006; 7: 14.
[41] Duscher D, Rennert RC, Januszyk M, Anghel E, Maan ZN, Whittam AJ, Perez MG, Kosaraju R, Hu MS, Walmsley GG, Atashroo D, Khong S, Butte AJ and Gurtner GC. Aging disrupts cell subpopulation dynamics and diminishes the function of mesenchymal stem cells. Sci Rep 2014; 4: 7144.
[42] Bolamperti S, Signo M, Spinello A, Moro G, Fraschini G, Guidobono F, Rubinacci A and Villa I. GH prevents adipogenic differentiation of mesenchymal stromal stem cells derived from human trabecular bone via canonical Wnt signaling. Bone 2018; 112: 136-144.
[43] Chen CY, Tseng KY, Lai YL, Chen YS, Lin FH and Lin S. Overexpression of insulin-like growth factor 1 enhanced the osteogenic capability of aging bone marrow mesenchymal stem cells. Theranostics 2017; 7: 1598-1611.